Journal of Inorganic Biochemistry 104 (2010) 126–135

Contents lists available at ScienceDirect

Journal of Inorganic Biochemistry

journal homepage: www.elsevier.com/locate/jinorgbio

Nitroimidazole conjugates of *bis*(thiosemicarbazonato)^{64}Cu(II) – Potential combination agents for the PET imaging of hypoxia

Paul D. Bonnitcha [a,1], Simon R. Bayly [a,*,1], Mark B.M. Theobald [a,1], Helen M. Betts [a,1], Jason S. Lewis [b,2], Jonathan R. Dilworth [a,1]

[a] Chemistry Research Laboratory, Department of Chemistry, University of Oxford, Mansfield Road, Oxford OX1 3TA, UK
[b] Department of Radiology, Washington University School of Medicine, St. Louis, MO 63110, USA

ARTICLE INFO

Article history:
Received 4 June 2009
Received in revised form 18 September 2009
Accepted 7 October 2009
Available online 24 October 2009

Keywords:
Molecular imaging
Radiochemistry
Copper-64
Bis(thiosemicarbazone)
Hypoxia

ABSTRACT

Combination agents comprising two different pharmacophores with the same biological target have the potential to show additive or synergistic activity. *Bis*(thiosemicarbazonato)copper(II) complexes (e.g. ^{64}Cu-ATSM) and nitroimidazoles (e.g. ^{18}F-MISO) are classes of tracer used for the delineation of tumor hypoxia by positron emission tomography (PET). Three nitroimidazole-*bis*(thiosemicarbazonato)copper(II) conjugates were produced in order to investigate their potential as combination hypoxia imaging agents. Two were derived from the known bifunctional *bis*(thiosemicarbazone) H_2ATSM/A and the third from the new precursor diacetyl-2-(4-*N*-methyl-3-thiosemicarbazone)-3-(4-*N*-ethylamino-3-thiosemicarbazone) – H_2ATSM/en. Oxygen-dependent uptake studies were performed using the ^{64}Cu radiolabelled complexes in EMT6 carcinoma cells. All the complexes displayed appreciable hypoxia selectivity, with the nitroimidazole conjugates displaying greater selectivity than a simple propyl derivative used as a control. Participation of the nitroimidazole group in the trapping mechanism is indicated by the increased hypoxic uptake of the 2- vs. the 4-substituted ^{64}Cu-ATSM/A derivatives. The 2-nitroimidazole derivative of ^{64}Cu-ATSM/en demonstrated superior hypoxia selectivity to ^{64}Cu-ATSM over the range of oxygen concentrations tested. Biodistribution of the radiolabelled 2-nitroimidazole conjugates was carried out in EMT6 tumor-bearing mice. The complexes showed significantly different uptake trends in comparison to each other and previously studied Cu-ATSM derivatives. Uptake of the Cu-ATSM/en conjugate in non-target organs was considerably lower than for derivatives based on Cu-ATSM/A.

1. Introduction

Hypoxia occurs to a variable extent in many solid tumors [1]. Its prominence in cancer is attributable to the impaired vasculature of tumors that occurs as a result of uncontrolled cell proliferation [2,3]. Clinical diagnosis of hypoxia is important because it is correlated with resistance to conventional therapeutic treatments and has a profound impact on patient survival [4]. Hypoxic tumors are often less susceptible to traditional chemotherapy [5] as a result of both limited drug penetration and induced resistance mechanisms [6,7]. Similarly, radiotherapy is usually far less effective in regions of hypoxia [8,9], mainly because oxygen is required to convert the initial DNA free radicals formed by ionisation into strand breaks [10]. Consequently there has been significant interest in developing non-invasive techniques for delineating hypoxia and a number of PET and SPECT agents have been developed for this purpose [11–16].

Nitroimidazoles and *bis*(thiosemicarbazonato)copper(II) complexes are two classes of hypoxia tracer that have been extensively investigated. It has been shown that 2-nitroimidazoles can be trapped in cells with low pO_2 values [17], and the 2-nitroimidazole compound [^{18}F]fluoromisonidazole (^{18}FMISO) has been used for PET imaging of stroke, ischemia myocardium and tumor hypoxia [12,18–20]. 2-Nitroimidazole cyclam derivatives radiolabelled with ^{99m}Tc, ^{64}Cu and ^{67}Cu have also been investigated as potential PET/SPECT agents for tumor hypoxia [21]. *Bis*(thiosemicarbazone) ligands derived from 1,2-diones form low molecular weight, neutral copper(II) complexes which are capable of rapid cellular uptake. Diacetyl-*bis*(N^4-methylthiosemicarbazonato)copper(II) (Cu-ATSM, where the positron emitting isotopes ^{60}Cu, ^{61}Cu or ^{64}Cu are used) has been shown to be selective for hypoxic tissue [22–24] and has been used clinically for the detection of hypoxia in cancer [25–27]. Both classes of tracer are thought to function via a redox trapping mechanism. Having crossed the cell

* Corresponding author. Tel.: +44 1865 285155; fax: +44 1865 272690.
E-mail address: simon.bayly@chem.ox.ac.uk (S.R. Bayly).
[1] Tel.: +44 (0)1865 285155; fax: +44 (0)1865 285002.
[2] Present address: Department of Radiology, Memorial Sloan-Kettering Cancer Center, 1275 York Avenue, NY 10065, USA.

0162-0134/$ - see front matter © 2009 Elsevier Inc. All rights reserved.
doi:10.1016/j.jinorgbio.2009.10.009

membrane, enzyme mediated reduction of the tracer molecule occurs. In cells with normal oxygen concentrations reoxidation by intracellular oxygen is rapid and the molecule can then leave the cell. In oxygen deprived environments, reoxidation is slow and decomposition of the molecule and/or additional reduction reactions occur leaving the radiolabelled fragments trapped in the cell. In the case of nitroimidazoles initial reduction to the radical anion is reversible, but subsequent reductions result in irreversible fragmentation [19,28]. With *bis*(thiosemicarbazonato)copper(II) complexes the initial reduction from Cu(II) to Cu(I) occurs reversibly, but the Cu(I) species formed is thought to become protonated and undergo decomplexation and trapping of the copper ion [24]. Derivatives such as Cu-ATSM that contain the diacetyl backbone show the best hypoxia selectivity and it has been suggested that this is due to their reduction being more reversible and occurring at a more negative reduction potential in comparison to other variants [29–31].

Bioconjugation is an attractive approach for improving the *in vivo* characteristics of hypoxia selective agents, since it has the potential to provide additional transport or targeting properties. For this reason we have been investigating strategies to introduce a functional group for conjugation into diacetyl-*bis*(N^4-methylthiosemicarbazones) without disrupting the diacetyl backbone or significantly altering the Cu(I/II) redox potential of the complex. The first derivative we developed which fulfils these requirements – H_2ATSM/A – utilizes a hydrazine group at one N-terminus [32]. A variety of ^{64}Cu-ATSM/A conjugates have been synthesized and we recently reported preliminary *in vitro* and *in vivo* results for a number of these. A series of lipophilic imine conjugates demonstrated significant hypoxia selectivity *in vitro* in EMT6 cells; however their uptake under normoxic conditions was considerably higher than that of Cu-ATSM [33]. *Ex vivo* biodistribution results from mice bearing EMT6 tumors showed high accumulation in the liver, suspected to be a consequence of the high lipophilicity or hydrolytic instability of the complexes. We have also studied a glucose conjugate of ^{64}Cu-ATSM/A [34]. This hydrophilic complex showed improved *in vitro* hypoxia selectivity in HeLa cells in comparison to ^{64}Cu-ATSM, due to a reduced level of uptake under normoxic conditions. *In vivo* results from PET imaging of rats bearing P22 carcino-sarcoma showed a similar pattern of biodistribution for both the ^{64}Cu-ATSM/A glucose conjugate and ^{64}Cu-ATSM. The significant effects of glucose conjugation were to exclude the tracer from the brain and shift its excretion pathway from primarily hepatointestinal to partially renal.

In principle nitroimidazole conjugates of *bis*(thiosemicarbazonato)copper(II) could show additive or synergistic selectivity for tumor hypoxia compared to their individual components. Interplay between the two differing redox trapping mechanisms might lead to properties such as a faster rate of uptake in hypoxic tissue, sensitivity to a broader range of oxygen concentrations or recognition of hypoxia in more diverse tumor types. In this paper we describe the synthesis of three *bis*(thiosemicarbazone)–nitroimidazole conjugates and their copper(II) complexes. Two of these are based on the previously described H_2ATSM/A platform. The third employs a novel bifunctional *bis*(thiosemicarbazone) – H_2ATSM/en – which possesses an ethylamino linker group. Radiolabelling with ^{64}Cu was carried out and the results of *in vitro* hypoxia selectivity and *ex vivo* biodistribution studies on the radiolabelled complexes are presented.

2. Materials and methods

2.1. General

All chemicals, unless otherwise stated, were purchased from Sigma–Aldrich Chemical Co. (St. Louis, MO, USA). Water was distilled and then deionized (18 MΩ/cm^2) by passing through a Milli-Q water filtration system (Millipore Corp., Milford, MA, USA). HPLC characterisation of the ligands and cold copper complexes was performed on a Hamilton-PRP1 reverse phase column, (4.1 mm × 150 mm, particle size 5 μm, SN 10843) with UV detection at λ = 254 nm using one of two gradient elution methods. Method A: 0.9 mL/min (MeCN/H_2O): start 5% MeCN, hold until 1 min, gradient to 95% MeCN at 15 min, hold until 25 min, reverse gradient to 5% MeCN at 30 min, hold to 35 min. Method B: 1.0 mL/min (MeCN/H_2O): start 5% MeCN, gradient to 95% MeCN at 15 min, hold until 20 min, gradient to 5% MeCN at 25 min, then hold until 30 min. NMR spectroscopy was performed on a Varian Mercury VX300 spectrometer (300 MHz), and spectra were referenced to the residual solvent peak. The splitting of proton resonances in the reported spectra is defined as s = singlet, d = doublet, t = triplet, q = quartet, m = multiplet, t = doublet of triplets, td = triplet of doublets, br = broad. Mass spectrometry (MS) was performed using a Bruker Micromass LCT time-of-flight mass spectrometer using electrospray ionisation with positive ion (ES^+) or negative ion (ES^-) detection. When possible high resolution mass spectrometry (HRMS) data was obtained and accurate masses are reported to four decimal places using tetraoctylammonium bromide (466.5352 Da) as an internal reference. Copper-64 was produced on a CS-15 biomedical cyclotron at the Washington University School of Medicine using published methods [35]. Radioactivity was counted with a Beckman Gamma 8000 counter containing a NaI crystal (Beckman Instruments, Inc., Irvine, CA, USA). HPLC characterisation of radiochemical compounds was performed on a Vydac Protein and Peptide column (C18 monomeric, 300 Å silica base, 4.6 mm × 100 mm) with UV detection and NaI scintillation crystal detection. A 25 min gradient elution method was employed (MeCN/H_2O, 0.1% TFA): start 0% MeCN hold until 5 min, gradient to 95% MeCN at 10 min, hold until 20 min, reverse gradient to 0% MeCN at 25 min, hold until 30 min. The retention time of the ^{64}Cu analogues were compared to those of the previously prepared copper analogues run under the same HPLC conditions. Radiochemical purity was tested radio-thin layer chromatography (radio-TLC) using 100 mm × 25 mm 250 μM reversed-phase hydrocarbon impregnated silica-gel plates with acetonitrile/water (4:1) as the mobile phase. In each case any unreacted copper remained at the origin (R_f: 0–0.1) while the radiolabelled complexes had R_f values of 0.8–0.9. TLC plates were analyzed on a BIOSCAN System 200 imaging scanner (Washington, DC, USA).

2.2. Synthesis

Boc-ethylenediamine [36], diacetyl-*bis*(N^4-methylthiosemicarbazonate) (H_2ATSM) [37], Cu-ATSM [24], 3-(4-nitroimidazol-1-yl) propionic acid [38], 3-(2-nitroimidazol-1-yl) propionic acid [39], diacetyl-2-(4-*N*-methyl-3-thiosemicarbazone) [32], and diacetyl-2-(4-*N*-methyl-3-thiosemicarbazone)-3-(4-*N*-amino-3-thiosemicarba-zone) (H_2ATSM/A) [32] were prepared by previously reported procedures.

2.2.1. Methyl-N-(2-^{t}butoxycarbonylaminoethyl)dithiocarbamate

Carbon disulphide (1.90 mL, 31.6 mmol) was added dropwise to a stirring solution of boc-ethylenediamine (5.06 g, 31.6 mmol) and triethylamine (4.41 mL, 31.6 mmol) in ethanol (100 mL) whilst maintaining the reaction at 25 °C with a water bath. After stirring for 90 min, iodomethane (1.97 mL, 31.6 mmol) was added and the resulting mixture stirred for a further 1¾ h. The solvent was removed and the residue re-suspended in ethyl acetate. This was washed with 1 M HCl (100 mL), sat. sodium bicarbonate solution (100 mL) and water (100 mL). The organic phase was dried ($MgSO_4$) and solvent removed under reduced pressure to give an off-white solid (7.10 g, 90%, 28.4 mmol). ^{1}H NMR (300 MHz,

$CDCl_3$): δ ppm 8.33 (1H, br s, NHC=S), 4.94 (1H, br s, NHBoc), 3.73 (2H, dt, $^3J_{HH}$ = 5.5, 5.2 Hz, CH_2NHC=S), 3.36 (2H, dt, $^3J_{HH}$ = 6.1, 5.5 Hz, CH_2NHBoc), 2.53 (3H, s, CH_3S), 1.39 (9H, s, Boc); MS (ES^+): m/z 273.1 $\{M + Na\}^+$ (100%).

2.2.2. 4-N-(2-^{t}butoxycarbonylaminoethyl)-3-thiosemicarbazide

A solution of methyl-*N*-(2-^{t}butoxycarbonylaminoethyl)dithiocarbamate (7.00 g, 27.9 mmol) and hydrazine hydrate (2.20 mL, ca. 38.5 mmol) was dissolved in ethanol (100 mL) and heated under reflux for 150 min. The solvent was removed under reduced pressure and the residue redissolved in chloroform (20 mL). This was passed through a plug of silica, washed with chloroform (20 mL) and the product eluted with methanol (30 mL). The methanol fraction was evaporated to provide an oil which solidified over a few days (6.24 g, 96%, 26.8 mmol). ^{1}H NMR (300 MHz, $CDCl_3$): δ ppm 7.76 (1H, br s, NHNH^2), 7.58 (1H, br s, CH_2NHC=S), 4.98 (1H, br s, CH_2NHBoc), 3.76 (2H, br s, NHNH_2), 3.69 (2H, dt, $^3J_{HH}$ = 6.3, 5.4 Hz, CH_2NHC=S), 3.32 (2H, dt, $^3J_{HH}$ = 6.0, 5.4 Hz, CH_2NHBoc), 1.38 (9H, s, Boc); $^{13}C\{^1H\}$ NMR (75.5 MHz, $CDCl_3$): δ ppm 182.6, 156.6, 79.6, 44.4, 40.1, 28.3; HRMS (ES^+): m/z (calcd) 257.1040 (257.1048) $\{M + Na\}^+$.

2.2.3. H_2ATSM/en-boc

4-*N*-(2-^{t}butoxycarbonylaminoethyl)-3-thiosemicarbazide (0.750 g, 3.21 mmol) was suspended in ethanol (30 mL) and stirred at 50 °C. Diacetyl-2-(4-methyl-3-thiosemicarbazone) (0.555 g, 3.21 mmol) was added in portions over 30 min. After the final addition, 2 drops of conc. HCl was added and the reaction heated under reflux for 3½ h. The cooled solution was poured into water (70 mL) to produce a white precipitate. This was collected by filtration, washed with water (2 × 30 mL) and diethyl ether (1 × 10 mL), and dried in vacuo to leave the product as a white solid (0.851 g, 2.07 mmol, 68%). ^{1}H NMR (300 MHz, DMSO-d_6) δ ppm 10.31 (1H, s, NHN=C), 10.29 (1H, s, NHN=C), 8.45 (1H, t, $^3J_{HH}$ = 5.1 Hz, CH_2NHC=S), 8.38 (1H, q, $^3J_{HH}$ = 4.5 Hz, CH_3NHC=S), 7.03 (1H, t, $^3J_{HH}$ = 5.1 Hz, NHBoc), 3.59 (2H, td, $^3J_{HH}$ = 5.4, 5.1 Hz, CH_2NHC=S), 3.17 (2H, td, $^3J_{HH}$ = 5.4, 5.1 Hz, CH_2NHBoc), 3.02 (3H, d, $^3J_{HH}$ = 4.55 Hz, CH_3NHC=S), 2.23 (3H, s, CH_3C=N), 2.21 (3H, s, CH_3C=N), 1.36 (9H, s, Boc); $^{13}C\{^1H\}$ NMR (75.5 MHz, DMSO-d_6): δ ppm 178.5, 178.0, 156.2, 148.3, 147.8, 77.9, 44.5, 39.1, 31.2, 28.2, 11.8, 11.7; HRMS (ES^+): m/z (calcd) 412.1555 (412.1565) $\{M + Na\}^+$. HPLC (Method B): R_t 12.37 min.

2.2.4. H_2ATSM/en

TFA (2 mL) was added to diacetyl-2-(4-*N*-methyl-3-thiosemicarbazone)-3-(4-*N*-^{t}butylethylcarbamate-3-thiosemicarbazone) (0.750 g, 1.93 mmol) and the resulting colourless solution stirred for 1½ h at room temperature. The solvent was removed to leave a sticky residue and sat. aqueous $NaHCO_3$ (10 mL) added slowly to produce a white suspension. After 20 min stirring at room temperature the solid was collected by filtration and washed with water (3 × 20 mL) and diethyl ether (2 × 20 mL). Drying in vacuo gave the product as off-white solid (0.431 g, 1.49 mmol, 77%). ^{1}H NMR (300 MHz, DMSO-d_6 with added TFA) δ ppm 10.53 (1H, d, $^3J_{HH}$ = 8.21 Hz, NHN=C), 10.24 (1H, d, $^3J_{HH}$ = 12.0 Hz, NHN=C), 8.50 (1H, q, $^3J_{HH}$ = 6.7 Hz, CH_3NHC=S), 8.39 (1H, t, $^3J_{HH}$ = 4.4 Hz, CH_2NHC=S), 7.87 (3H, br s, NH_3^+), 3.83 (2H, td, $^3J_{HH}$ = 6.1, 5.9 Hz, CH_2NHC=S), 3.05 (2H, tq, $^3J_{HH}$ = 6.3, 6.1 Hz, $CH_2NH_3^+$), 3.02 (3H, d, $^3J_{HH}$ = 6.3 Hz), CH_3NHC=S), 2.22 (6H, br s, 2 × CH_3C=N); $^{13}C\{^1H\}$ NMR (75.5 MHz, DMSO-d_6): δ ppm 178.4, 177.6, 147.6 (2 carbons), 46.3, 40.3, 31.2, 11.7, 11.5; HRMS (ES^+): m/z (calcd) 290.1228 (290.1222) $\{M + H\}^+$; HPLC (Method B, run with 0.1% TFA): R_t 6.08 min.

2.2.5. Zn-ATSM/en

$Zn(OAc)_2{\cdot}2H_2O$ (0.23 g, 1.0 mmol) was added to a solution of H_2ATSM/en (0.25 g, 0.86 mmol) in methanol (10 mL) and the mixture stirred at room temperature. for 1 h. Water (20 mL) and triethylamine (1 mL) were added causing the formation of a yellow precipitate. The solution was filtered, the solid washed with water and diethyl ether and dried in vacuo to give the product as a yellow solid (0.29 g, 0.69 mmol, 80%). The ^{1}H NMR (300 MHz, DMSO-d_6) gave broad peaks possibly due to protic equilibria or self-association in solution; δ ppm 7.32 (1H, br s), 7.16 (1H, br s), 3.27 (2H, br m) 2.82 (3H, d, $^3J_{HH}$ = 3.5 Hz) 2.42 (2H, br m), 2.22 (3H, s), 2.14 (3H, s). HRMS (ES^+): m/z (calcd) 352.0362 (352.0356) $\{M + H\}^+$; Crystals suitable for X-ray diffraction were grown by the diffusion of H_2O into a DMSO solution of the product. The complete crystallographic data can be obtained at http://www.ccdc.cam.ac.uk/ (deposition number: CCDC 710238).

2.2.6. N-hydroxysuccinimide propanoate

This procedure was adapted from the procedure of Hirata et al. [40] DCC (8.00 g, 38.9 mmol) was added to a solution of *N*-hydroxysuccinimide (4.60 g, 40.0 mmol) and propionic acid (3.00 mL, 39.5 mmol) in THF (100 mL) and the mixture stirred at −78 °C for 1 h. After stirring for a further 2 h at room temperature, the solution was filtered, the solvent removed and the residue partitioned between dichloromethane and water. The organic layer was washed with a sat. $NaHCO_3$ solution (2 × 25 mL), dried with $MgSO_4$ and the solvent removed to leave *N*-hydroxysuccinimide propanoate as a viscous oil which solidified to a white solid over a few hours (5.13 g, 30.0 mmol, 77%). ^{1}H NMR (300 MHz, DMSO-d_6): δ ppm 2.76 (4H, s, CH_2–N(–O)–CH_2), 2.66 (2H, q, $^3J_{HH}$ = 7.5 Hz, O=C–CH_2CH_3), 1.11 (3H, t, $^3J_{HH}$ = 7.5 Hz, O=C–CH_2CH_3); $^{13}C\{^1H\}$ NMR (75.5 MHz, DMSO-d_6): δ ppm 171.1, 170.8, 25.4, 24.3, 9.8; MS (EI+): 171.1 (5%, $\{M\}^+$), 87.1 (60%, $\{M–(O=C–CH_2–CH_2–C=O)\}^+$), 57.0 (100%, $\{M–(N\text{-hydroxysuccinimide})\}^+$).

2.2.7. N-hydroxysuccinimide 3-(4-nitroimidazol-1-yl)propanoate

EDC (520 mg, 2.80 mmol) was added to a mixture of *N*-hydroxysuccinimide (320 mg, 2.78 mmol) and 3-(4-nitroimidazol-1-yl) propionic acid (500 mg, 2.75 mmol) in THF (25 mL) and the mixture stirred for 1 h at −78 °C. The mixture was stirred for a further by 15 h at room temperature before the solvent was removed and water/methanol (1:1, 10 mL) added to the residue. The resulting solid collected, cold water (2 mL) and diethylether (2 × 20 mL) to leave pure *N*-hydroxysuccinimide 3-(4-nitro-1H-imidazol-1-yl) propanoate as a white solid (611 mg, 2.16 mmol, 80%). ^{1}H NMR (300 MHz, DMSO-d_6): δ ppm 8.44 (1H, d, $^3J_{HH}$ = 1.4, imidazole), 7.87 (1H, d, $^3J_{HH}$ = 1.3, imidazole), 4.40 (2H, t, $^3J_{HH}$ = 6.8), 3.40 (2H, t, $^3J_{HH}$ = 6.8, O=C–CH_2CH_2-imidazole), 2.76 (4H, s, CH_2–N(–O)–CH_2); $^{13}C\{^1H\}$ NMR (75.5 MHz, DMSO-d_6): δ ppm 170.8, 167.5, 147.7, 138.2, 122.3, 42.8, 32.0, 25.9; HRMS (ES^+): m/z (calc) 283.0684 (283.0679) $\{M + H\}^+$. Elem. Anal.(%): Found: C 42.5, H 3.6, N 19.8, Calc. (for $C_{10}H_{10}N_4O_6$): C 42.6, H 3.6, N 19.9. HPLC (Method A): R_t 8.00 min.

2.2.8. H_2**L^1**

Triethylamine (150 μL, 1.07 mmol) was added to a solution of H_2ATSM/A (260 mg, 1.00 mmol) in DMSO (3 mL), followed by *N*-hydroxysuccinimide 3-(4-nitroimidazol-1-yl)propanoate (296 mg, 1.05 mmol). The solution was stirred for 6 h, water (20 mL) added, the solution centrifuged and the crude solid collected. The solid was then washed with ethanol (10 mL) and diethylether (3 × 10 mL) to leave H_2**L^1** as an off-white solid (358 mg, 0.84 mmol, 84%). ^{1}H NMR (300 MHz, DMSO-d_6): δ ppm 10.41 (H, s, S=C–NH–NH–C=O), 10.11 (2H, br s, 2 × S=C–NH–N) 9.99 (H, s, S=C–NH–NH–C=O), 8.37 (2H, m, NH–CH_3 and imidazole), 7.83 (H, s, imidazole), 4.35 (2H, t, $^3J_{HH}$ = 6.7 Hz, O=C–CH_2–CH_2-imidaz-

ole), 3.02 (3H, s, CH_3-NH) 2.80 (2H, t, $^3J_{HH}$ = 6.7 Hz, O=C–CH_2–CH_2-imidazole), 2.24 (3H, s, N=C–CH_3), 2.17 (3H, s, N=C–CH_3); $^{13}C\{^1H\}$ NMR (75.5 MHz, DMSO-d_6): δ ppm 180.2, 179.0, 168.7, 150.7, 148.1, 147.5, 138.3, 122.5, 44.3, 34.0, 32.2, 12.4, 12.2; MS (ES^-) m/z: 427.1 $\{M-H\}^-$ (100%); HPLC (Method A): R_t 8.69 min. Elem. Anal.(%): Found: C 34.7, H 5.0, N 31.2. Calc. (for $H_2\mathbf{L^1}\cdot H_2O$, $C_{13}H_{22}N_{10}O_3S_2$): C 35.0, H 5.0, N 31.4.

2.2.9. $H_2\mathbf{L^2}$

3-(2-Nitroimidazol-1-yl)propionic acid (88 mg, 0.48 mmol) and then BOP (200 mg, 0.47 mmol) were added to a solution of H_2ATSM/A (100 mg, 0.38 mmol) and DIPEA (100 μL, 0.59 mmol) in DMF (3 mL). After stirring for 12 h, water (20 mL) was added, the precipitate collected and washed with ethanol (5 mL) and ether (3 × 20 mL) to leave $H_2\mathbf{L^2}$ as an off-white solid (131 mg, 0.31 mmol, 81%). ^{1}H NMR (300 MHz, DMSO-d_6): δ ppm 10.30 (H, s, S=C–NH–NH–C=O), 10.18 (2H, br s, 2 × S=C–NH–N), 9.91 (H, s, S=C–NH–NH–C=O), 8.40 (H, s, NH–CH_3), 7.49 (H, s, imidazole), 7.15 (H, s, imidazole), 4.60 (2H, t, $^3J_{HH}$ = 6.6 Hz, O=C–CH$_2$–CH_2-imidazole), 3.02 (3H, s, CH_3-NH), 2.75 (2H, t, $^3J_{HH}$ = 6.6 Hz, O=C–CH_2–CH$_2$-imidazole), 2.22 (3H, s, N=C–CH_3), 2.16 (3H, s, N=CH_3); $^{13}C\{^1H\}$ NMR (75.5 MHz, DMSO-d_6): δ ppm: 180.5, 178.1, 168.6, 150.4, 148.1, 145.5, 128.2, 128.0, 44.3, 35.0, 31.2, 12.2, 11.9; MS (ES^-) m/z: 427.1 $\{M-H\}^-$ (100%); HPLC (Method A): R_t 8.57 min. Elem. Anal.(%): Found: C 34.6, H 5.0, N 31.3. Calc. (for $H_2\mathbf{L^2}\cdot H_2O$, $C_{13}H_{22}N_{10}O_3S_2$): C 35.0, H 5.0, N 31.4.

2.2.10. $H_2\mathbf{L^3}$

As $H_2\mathbf{L^2}$, except using H_2ATSM/en (110 mg, 0.38 mmol), DIPEA(100 μL, 0.59 mmol), BOP (200 mg, 0.47 mmol), DMF (3 mL) and 3-(2-nitroimidazol-1-yl) propionic acid (90 mg, 0.49 mmol) to give $H_2\mathbf{L^3}$ as a white solid (122 mg, 0.27 mmol, 71%). ^{1}H NMR (300 MHz, DMSO-d_6): δ ppm 10.28 (2H, br s, 2 × S=C–NH–N), 8.40 (2H, br s, CH$_3$–NH, CH$_2$–NH–C=S), 8.19 (H, s, NH–C=O), 7.49 (H, s, imidazole), 7.15 (H, s, imidazole), 4.60 (2H, t, $^3J_{HH}$ = 6.8 Hz, O=C–CH$_2$–CH_2-imidazole), 3.58 (2H, t, $^3J_{HH}$ = 6.0 Hz, S=C–NH–CH_2–CH$_2$–NH–C=O), 3.02 (5H, m, S=C–NH–CH$_2$–CH_2–NH–C=O, CH_3–NH), 2.75 (2H, t, $^3J_{HH}$ = 6.8 Hz, O=C–CH_2–CH$_2$-imidazole), 2.18 (6H, s, 2 × N=C–CH_3); $^{13}C\{^1H\}$ NMR (75.5 MHz, DMSO-d_6): δ ppm: 179.1, 178.4, 10.3, 148.9, 148.2, 145.5, 128.2, 128.0, 46.5, 44.3, 38.2, 36.2, 31.9 11.8, 11.7; MS (ES^-) m/z: 455.1 $\{M-H\}^-$ (100%); HPLC (Method A): R_t 9.10 min. Elem. Anal.(%): Found: C 37.9, H 5.4, N; 29.5. Calc. (for $H_2\mathbf{L^3}\cdot H_2O$, $C_{15}H_{26}N_{10}O_4S_2$): C 38.0, H 5.5, N 29.5.

2.2.11. $H_2\mathbf{L^4}$

As $H_2\mathbf{L^1}$, except using triethylamine (150 μL, 1.07 mmol), H_2ATSM/A (260 mg, 1.00 mmol) and *N*-hydroxysuccinimide propanoate (178 mg, 1.05 mmol) and DMSO (3 mL). $H_2\mathbf{L^4}$ was isolated as a white solid (250 mg, 0.69 mmol, 69%). ^{1}H NMR (300 MHz, DMSO-d_6): δ ppm 10.50 (H, s, S=C–NH–NH–C=O, 10.20 (H, s, S=C–NH–NH–C=O), 9.99 (H, br s, S=C–NH–N), 9.93 (H, br s, S=C–NH–N), 8.39 (H, s, NH–CH$_3$), 3.02 (3H, s, CH_3-NH), 2.20 (8H, m, 2 × N=CH_3 and CH_2–CH$_3$), 1.07 (3H, t, $^3J_{HH}$ = 7.5 Hz, CH$_2$–CH_3). $^{13}C\{^1H\}$ NMR (75.5 MHz, DMSO-d_6): δ ppm 180.2, 179.0, 168.7, 150.7, 148.1, 32.2, 24.0 12.7, 12.1, 9.8; HRMS (ES^-) m/z: 361.1011 (361.1014) $\{M-H\}^-$; HPLC (Method A): R_t 8.13 min. Elem. Anal.(%): Found: C 35.8, H 6.4, N 28.8. Calc. (for $H_2\mathbf{L^4}\cdot H_2O$, $C_{10}H_{21}N_7O_2S_2$): C 35.8, H 6.3, N 29.2.

2.2.12. Complex **1**

$CuCl_2\cdot 2H_2O$ (94 mg, 0.55 mmol) in DMF (3 mL) was added dropwise over 5 min to a stirring solution of $H_2\mathbf{L^1}$ (214 mg, 0.5 mmol) in DMF (2 mL). After 20 min, water (30 mL) was added to the solution, the mixture centrifuged if necessary, and the solid residue collected. The solid was washed with water (20 mL), cold ethanol (5 mL), ether (2 × 20 mL) and dried in vacuo to give Compound 1 as a deep red–brown solid (85%). HRMS (ES^+): m/z (calcd) 490.0387 (490.0379) $\{M+H\}^+$; HPLC (Method A): R_t 9.37 min. Elem. Anal.(%): Found: C 31.6, H 3.7, N 28.4. Calc. (for Cu$\mathbf{L^1}$, $C_{13}H_{18}CuN_{10}O_3S_2$): C 31.9, H 3.7, N 28.6.

2.2.13. Complex **2**

As complex **1**, except with $CuCl_2\cdot 2H_2O$ (47 mg, 0.28 mmol) in DMF (2 mL) and $H_2\mathbf{L^2}$ (107 mg, 0.25 mmol) in DMF (2 mL). Compound **3** was obtained as a red/brown solid (104 mg, 0.20 mmol, 80%). HRMS (ES^+): m/z (calcd) 490.0380 (490.0379) $\{M+H\}^+$; HPLC (Method A) R_t: 9.44 min. Elem. Anal.(%): Found: C 31.6, H 3.7, N 28.4. Calc. (for Cu$\mathbf{L^2}$, $C_{13}H_{18}CuN_{10}O_3S_2$): C 31.9, H 3.7, N; 28.6.

2.2.14. Complex **3**

As complex **1**, except with $CuCl_2\cdot 2H_2O$ (47 mg, 0.28 mmol) in DMF (2 mL) and $H_2\mathbf{L^3}$ (114 mg, 0.25 mmol) in 2 mL DMF. Compound **4** was obtained as a red solid (104 mg, 0.20 mmol, 80%). MS (ES^+): m/z 517.1 $\{M+H\}^+$ (100%); HPLC (Method A) R_t: 10.21 min. Elem. Anal.(%): Found: C 34.6, H 4.4, N 26.8. Calc. (for Cu$\mathbf{L^3}$, $C_{15}H_{22}CuN_{10}O_3S_2$): C 34.8, H 4.3, N 27.0.

2.2.15. Complex **4**

As complex **1**, except with $CuCl_2\cdot 2H_2O$ (94 mg, 0.55 mmol) in DMF (3 mL) and $H_2\mathbf{L^4}$ (180 mg, 0.50 mmol) in DMF (3 mL). Compound 2 was isolated as a deep brown–red solid (285 mg, 0.38 mmol 75%). HRMS (ES^+): m/z (calcd) 379.0310 (379.0310) $\{M+H\}^+$; HPLC (Method A) R_t: 9.37 min. Elem. Anal.(%): Found: C 31.4, H 4.7, N 26.7. Calc. (for Cu$\mathbf{L^4}$, $C_{10}H_{17}CuN_7OS_2$): C 31.7, H 4.5, N 27.0.

2.3. Cyclic voltammetry

Cyclic voltammetry experiments were performed on a CH instruments 600A electrochemical analyser with Chi600 software, a platinum working electrode, a platinum wire supporting electrode and a Ag|$AgNO_3$ reference electrode. Scans were internally referenced to ferrocene (0.53 V vs. SCE). Solutions of the respective complexes were prepared to approximately 1 mM in degassed DMF containing 0.1 M TBA[BF_4] and were run between 0.3 and −1.6 V (vs. SCE) at a scan rate of 100 mV/s.

2.4. ^{64}Cu complexation of ligands

All ligands, with the exception of $H_2\mathbf{L^3}$ were labelled with ^{64}Cu in an identical fashion. The ligand was dissolved in DMSO to give an overall concentration of 0.1 mg/mL. A total of 200 μL (20 μg) of this solution was then added to 200 μL (10 mCi) of ^{64}Cu in chelexed NaOAc buffer (0.1 M), which was typically supplied at a specific activity of around 200 mCi/μg. This solution was then stirred for 30 min at 37 °C, after which it was loaded onto a C18 SepPak-Light® (Waters Corporation, Milford, MA), which had been conditioned with 5 mL of ethanol and 5 mL of water. After loading the sample, 15 mL of water was passed through to remove the DMSO and any unreacted ^{64}Cu. The labelled complexes were then eluted in 350 μL of ethanol (following a 150 μL ethanol elution for the void volume). The radiochemical yield for all radiolabelling reactions was 80–85% and were all purified to >95% purity. Complex **3** was radiolabelled in a similar fashion, except the stock $^{64}Cu^{2+}$ solution was prepared in pH 4.5 acetate buffer (0.1 M).

2.5. Partition coefficients

Octanol/water partition coefficients were calculated as log-*P* = log(counts in octanol/counts in PBS buffer (pH 7.4)) and were determined in triplicate as described previously [41].

2.6. Media stability

To measure the stability of the labelled complexes, 5 μCi of the required ^{64}Cu complex was incubated in 1 mL of media at 37 °C, where at 1, 5, 15, 30 and 60 min the proportion of intact complex was determined using radio-TLC.

2.7. Serum protein binding

To measure the stability of the labelled complexes, 5 μCi of the required ^{64}Cu complex was incubated in 1 mL of fresh mouse serum at 37 °C. At 1, 5, 15, 30 and 60 min triplicate 50 μL fractions were removed and 200 μL of ethanol added to each to precipitate the proteins present. The sample was then centrifuged until the precipitated proteins formed a pellet. The supernatant was removed from the pellet and the pellet washed with 500 μL ethanol, and the sample centrifuged again. The combined supernatants and the pellet were counted on a gamma counter and the percentage protein-bound ^{64}Cu calculated.

2.8. In vitro hypoxia selectivity

The apparatus and procedures used for these *in vitro* experiments are based on those previously described [23,42]. The apparatus controls the *in vitro* incubation conditions of temperature, humidity, pH, and oxygen tension.

2.8.1. Anoxia vs. normoxia

Two 10 mL aliquots were taken from a homogenous cell suspension of EMT6 mammary carcinoma cells (50 mL, 5×10^6 cells/mL) and each was equilibrated in a three-necked, glass round-bottomed flask at 37 °C under either anoxic (95% N_2, 5% CO_2) or normoxic (75% N_2, 20% O_2, 5% CO_2) conditions by passing a continuous flow of warmed humidified gas over the cells. The flasks were shaken throughout the experiment. After 30 min, when the oxygen concentration in the vessels had reached equilibrium, 50 μCi of the ^{64}Cu-labelled complex was added. At 1, 5, 15, 30 and 60 min, triplicate 200 μL samples of cell suspension were removed, and centrifuged to pellet the cells. The percentage cellular uptake of the radiolabelled compound was calculated as described previously [23,29]. As a control, the compounds were put through the identical methods without cells present to determine the extent to which the compounds adhere to vials due to the lipophilicity of the compounds. No appreciable adherence of any of the compounds was noted.

2.8.2. Oxygen concentration study

Aliquots (10 mL) of a homogenous cell suspension of EMT6 mammary carcinoma cells (5×10^6 cells/mL) were equilibrated as above in three-necked, glass round-bottomed flasks at 37 °C at various oxygen concentrations (0%, 0.1%, 0.5%, 5%, or 20%). The flasks were shaken throughout the experiment. The gases used were 5% CO_2, the desired percentage of O_2, and the balance N_2. After 30 min, when the vessels had reached equilibrium, 50 μCi of the ^{64}Cu-labelled complex was added. At 15 min, triplicate samples of 200 μL of cell suspension were removed and centrifuged to pellet the cells. The percentage accumulation of the compound into the cells was then calculated. As a control, this experiment was performed with ^{64}Cu-ATSM and ^{64}Cu(acetate)$_2$.

2.9. Ex vivo biodistribution

All animal experiments were conducted in compliance with the Guidelines for the Care and Use of Research Animals established by Washington University's Animal Studies Committee. The biodistribution studies were conducted in female BALB/c mice (20 g, aged 5–6 weeks) (Charles River Laboratories, Wilmington, MA) that had been implanted with 6×10^5 EMT6 cells in 100 μL medium into the right flank. The tumors were allowed to grow for 12-days post implantation, at which time the animals received 10 μCi of the desired complex in 100 μL of a saline/ethanol mix (ethanol < 5%) via lateral tail-vein injection. The animals were euthanized at desired time points (5, 20, 60 min, $n = 4$ per group) and the organs harvested (blood, lung, liver, spleen, kidney, heart, brain, bone, tumor, and intestines). Once the tissues and organs of interest were removed they were weighed and the radioactivity was measured in a γ-counter. The percent dose per gram (%ID/g) and percent dose per organ (%ID/organ) were then calculated by comparison to known standards.

2.10. Statistical methods

To compare the differences in cell uptake and biodistribution, Student's *t* test was performed. Differences at the 95% confidence level ($P < 0.05$) were considered significant.

3. Results and discussion

3.1. Chemistry

The target *bis*(thiosemicarbazonato)copper(II)–nitroimidazole conjugates **1**–**3** and their ^{64}Cu labelled analogues were prepared directly from their respective proligands $H_2\mathbf{L^1}$–$H_2\mathbf{L^3}$. Complex **1** incorporates 4-nitroimidazole, whereas **2** and **3** use 2-nitroimidazole, which, of the two isomers, has been shown to possess superior hypoxia selectivity (Scheme 1). The amide linkage was used (rather than the previously studied imine) to tether the nitroimidazole group to the bifunctional *bis*(thiosemicarbazone) in order to lessen the likelihood of hydrolysis under biological conditions. A simple propyl conjugate **4** (Scheme 1), was produced (via $H_2\mathbf{L^4}$) in order to model any structural and electronic effects due to the amide linkage and allow proper assessment of the effect of the nitroimidazole group on the properties of **1** and **2**. $H_2\mathbf{L^1}$ and $H_2\mathbf{L^4}$ were prepared by reaction of H_2ATSM/A with the *N*-hydroxysuccinimide esters of 3-(4-nitroimidazol-1-yl)propionic acid and propionic acid respectively (Scheme 2). However this method proved to be unsuitable for coupling with the 3-(2-nitroimidazol-1-yl)propionic acid, and gave a number of intractable products. Synthesis of $H_2\mathbf{L^2}$ was achieved by direct coupling of H_2ATSM/A with 3-(2-nitro-

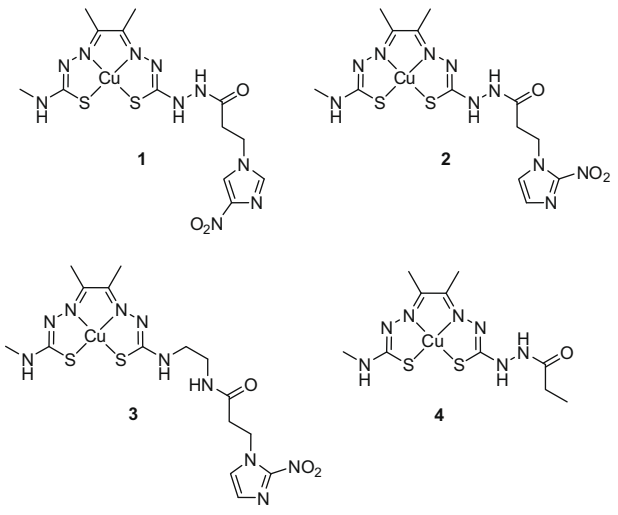

Scheme 1. *Bis*(thiosemicarbazonato)copper(II)–nitroimidazole conjugates in this study.

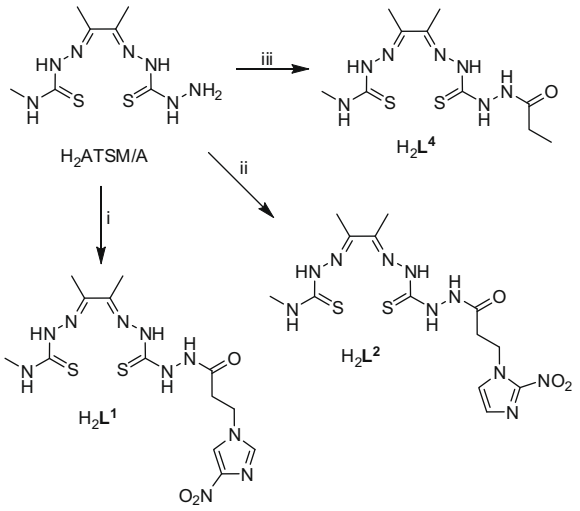

Scheme 2. Synthesis of H_2ATSM/A derivatives. (i) *N*-hydroxysuccinimidyl-3-(4-nitro-1*H*-imidzol-1-yl)propanoate, Et_3N, DMSO; (ii) 3-(2-nitro-1*H*-imidzol-1-yl)propionic acid, BOP, DIPEA, DMF and (iii) *N*-hydroxysuccinimidyl propanoate, Et_3N, DMSO.

imidazol-1-yl)propionic acid using the BOP reagent. In order to probe the effect of the hydrazine linker on the properties of complexes based on H_2ATSM/A, we devised a new bifunctional *bis* (thiosemicarbazone) – H_2ATSM/en (Scheme 3) – with an aminoethyl tethering group. Boc-1,2-diaminoethane was converted to the corresponding thiosemicarbazide by conversion to the methyl dithiocarbamate and subsequent hydrazinolysis. The 4-(boc-2-ethylamino)-3-thiosemicarbazide was condensed with diacetyl-2-(4-*N*-methyl-3-thiosemicarbazone) to produce the H_2ATSM/en-boc. Treatment with neat TFA gave H_2ATSM/en. Reaction of H_2ATSM/en with $Zn(OAc)_2$ gave the complex Zn-ATSM/en. Single crystals of this complex were grown by diffusion of atmospheric water into a DMSO solution and X-ray structure determination carried out (see supporting information). Synthesis of $H_2\mathbf{L^3}$ was achieved by direct coupling of H_2ATSM/en with 3-(2-nitroimidazol-1-yl)propionic acid using BOP.

The cold copper compounds were prepared by reaction of the appropriate free ligand with 1.1 equivalents of $CuCl_2{\cdot}2H_2O$ in

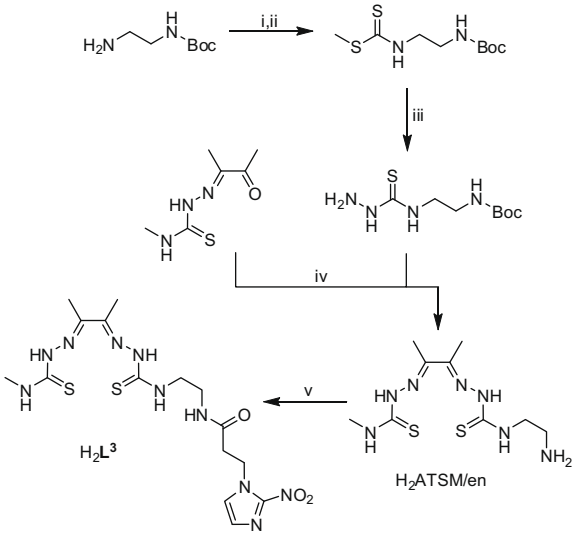

Scheme 3. Synthesis of H_2ATSM/en and $H_2\mathbf{L^4}$. (i) CS_2, Et_3N, EtOH; (ii) MeI; (iii) H_2N_2, EtOH; (iv) HCl, EtOH; and (v) 3-(2-nitro-1*H*-imidzol-1-yl)propionic acid, BOP, DIPEA, DMF.

DMF at room temperature. The ^{64}Cu complexes were prepared by the direct reaction of $^{64}Cu(OAc)_2$ with the corresponding proligand ($H_2\mathbf{L^1}$–$H_2\mathbf{L^4}$), and their identity confirmed by HPLC co-injection of the radiolabelled complex with the authentic non-radioactive analogue and comparison of the HLPC retention times (R_t values were within ±5%). A summary of the HPLC data is shown in Table 2. In a number of previous studies ^{64}Cu-radiolabelling *via* transmetallation of the *bis*(thiosemicarbazonato)Zn(II) complex was used, since it resulted in complexes of higher radiochemical purity than direct labelling. It has recently been demonstrated that this method in combination with novel a solid phase purification technique which selectively extracts the Zn(II) precursor by axial coordination could be used to produce tracers of higher specific activity [43]. Such purification methods were not required in this study since direct labelling of the *bis*(thiosemicarbazone) ligands resulted in sufficient radiochemical purity (>95% as determined by radio-TLC) and specific activity (specific activities of 200–500 mCi/mg ligand and 40–50 mCi/mg ligand were used for biodistribution studies and cell culture studies respectively).

3.2. Electrochemistry

Cyclic voltammograms were measured for complexes **1**–**4** and Cu-ATSM in DMF solution, scanning from 0.3 V to −1.6 V (all potentials measured vs. SCE). All the complexes displayed a quasi-reversible reduction wave centered at approximately −0.60 V (Table 1), which is attributed to the Cu(I/II) redox couple. The most negative redox potentials were observed for Cu-ATSM and **3** (−0.64 V and −0.63 V respectively). The reversibility of the copper(I/II) couple was also measurably higher in these two complexes, with the separation between the cathodic and anodic peaks being between 0.21 and 0.25 V for complexes **1**, **2** and **4**, whereas the peak separation was 0.12 V for **3** and 0.10 V for Cu-ATSM. In addition to the metal centered reduction, complexes **1**–**3** each displayed a further, quasi-reversible reduction process at a more negative potential. These occur at approximately −1.3 V (for the 4-nitroimidazole compound, **1**) and −1.0 V (for the 2-nitroimidazoles **2** and **3**) and are attributed to reduction of the nitroimidazole group. The electrochemistry of nitroimidazoles has been described in detail elsewhere [44,45].

3.3. Lipophilicity measurements

The partition coefficients (log *P*) for the compounds are displayed in Table 2. Complexes **1** and **2**, which differ only by the position of nitro group of the nitroimidazole, have very similar log *P* values (1.13 ± 0.02 and 1.11 ± 0.03 respectively), which is unsurprising given the similarities of their structures. Model complex **4** is more lipophilic (log *P* = 1.33 ± 0.05), as is **3** (log *P* = 1.45 ± 0.01), which contains the ethylenediamine linker. ^{64}Cu-ATSM is significantly more lipophilic than any of the amide conjugates used in this study (log *P* = 1.85 ± 0.05) [33].

Table 1
Copper (I/II) redox potentials as determined by cyclic voltammetry. Studies were performed in degassed DMF with 0.1 M [TBA][BF_4] at a scan rate of 100 mV/s. Ferrocene was used as an internal reference. All values are in volts relative to SCE.

Complex	$E_{½}$	E_p	E_p	ΔE
Cu-ATSM	−0.64	−0.69	−0.59	0.10
1	−0.58	−0.68	−0.47	0.21
2	−0.57	−0.69	−0.45	0.24
3	−0.63	−0.69	−0.57	0.12
4	−0.58	−0.70	−0.45	0.25

Table 2
Partition coefficients (Log *P*), HPLC R_t values (min) and TLC R_f values.

Complex	Log *P*[a]	R_t	R_t (^{64}Cu)	R_f[b]
1	1.13 ± 0.02	12.96	13.24	0.84
2	1.11 ± 0.03	13.16	13.25	0.84
3	1.45 ± 0.01	13.25	13.36	0.82
4[c]	1.33 ± 0.05	13.32	13.46	0.86

[a] The Log *P* value of ^{64}Cu-ATSM under these conditions has previously been determined to be 1.85 ± 0.05.
[b] Reverse phase TLC (C18) using 80:20 acetonitrile:water.
[c] HPLC performed without 0.1% TFA in mobile phase.

3.4. Serum protein binding and media stability

Compounds **1**–**4** were incubated for 60 min in fresh mouse serum with samples taken at various time points. All compounds displayed similar results, with approximately 20% of the activity bound to proteins after 1 min. This remained constant at all timepoints over the remaining 60 min. These results are comparable to the previously observed for Cu-ATSE in mouse serum, and the previously studied H_2ATSM/A imine and glucose conjugates [33,46]. No appreciable decomposition was detected for any of the radiotracers in serum-free media over the same time period.

3.5. Cell uptake studies

The apparatus used in these *in vitro* experiments has been used in previous hypoxia selectivity studies [23,46], and is specifically designed to keep variables such as cell concentration, temperature and pH constant. The uptake profiles for compounds **1**–**4** in EMT6 cells under both anoxic and normoxic conditions over 60 min are displayed in Fig. 1. All the compounds showed hypoxia selectivity, with statistically significant differences in cellular uptake between normoxic and hypoxic conditions at all time points ($P \leqslant 0.05$). Considerable variation in the cellular uptake and degree of hypoxia selectivity was observed between the complexes. The model complex **4** showed 69.0 ± 2.1% cellular uptake under anoxic conditions after 1 min which increased to 85.6 ± 0.6% at 30 min and remained at a similar level thereafter. Uptake under normoxic conditions was significantly lower, but followed a similar profile, with 38.5 ± 1.7% uptake after 1 min, increasing to 64.8 ± 0.8% at 30 min and level thereafter. At 60 min the hypoxia selective index (HSI) value [30] of **4** was 0.51. The level of uptake is slightly lower under both normoxic and anoxic conditions than observed with previously studied imine conjugates using an identical experimental set-up [33]. The imine conjugates are considerably more lipophilic than **4** and it is likely that their higher cellular uptake is due to superior membrane permeability.

The 4-nitroimidazole, **1** showed a markedly different uptake profile, and lower overall uptake compared to both **4** and the previously studied imine conjugates. Uptake for **1** under anoxic conditions was 22.5 ± 0.8% after 1 min, and increased to 45.6 ± 0.8% at 60 min. Under normoxic conditions uptake was 16.6 ± 0.7% after 1 min and remained at a similar level over the time course of the experiment. The HSI of **1** at 60 min was 0.64, somewhat higher than for **4**. Thus the addition of the bio-reducible nitroimidazole group to the *bis*(thiosemicarbazonato)Cu(II) complex appears to lead to an increase in hypoxia selectivity at the expense of a reduction in cell permeability. One factor causing the latter effect could be the lower lipophilicity of **1** (log *P* = 1.13) compared to **4** (log *P* = 1.33).

The 2-nitroimidazole, **2** showed a similar uptake profile to its 4-nitroimidazole analogue **1**. The observed uptakes of 64.5 ± 1.3% and 26.2 ± 1.7% at 60 min under anoxic and normoxic conditions respectively, correspond to an HSI of 0.71. The enhanced selectivity of **2** compared to **1** is due to greater accumulation in anoxic cells. It therefore appears that this small change in substitution generates increased hypoxia selectivity. Lipophilicity is unlikely to be a factor since the log *P* of **2** (1.11) is similar to that of **1**. However previous work has shown that the reduction potential of the nitro group in 2-nitroimidazoles is less negative than that of 4-nitroimidazoles. This is thought to lead to the superior hypoxia selectivity observed

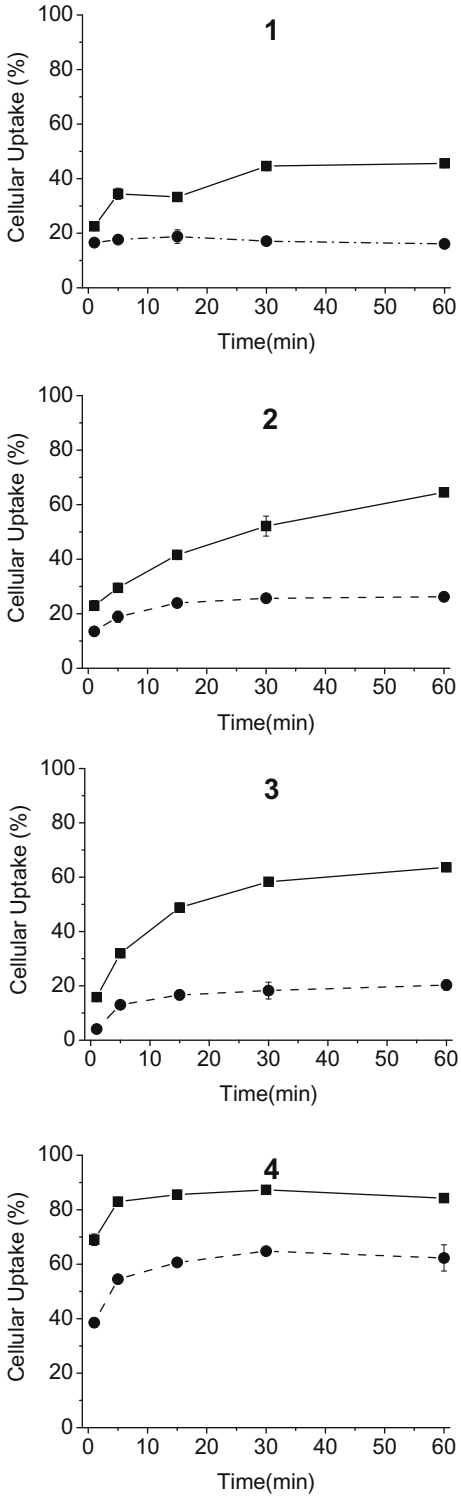

Fig. 1. Graphs showing uptake of radiolabelled complexes **1**–**4** in EMT6 cells under normoxic (dashed line) and anoxic (solid line) conditions. Errors (one stan. dev.), if not indicated, are within symbols.

with 2-nitroimidazole derivatives compared to their 4-nitroimidazole analogues [47]. The cyclic voltammetry results confirm that the reduction potentials of the 2-nitroimidazole groups in **2** and **3** are less negative (by 300 mV) than that of the 4-nitroimidazole in **1**. Taking this into account the increased uptake of **2** in anoxic cells is a strong indication that the nitroimidazole is playing an active role in the redox trapping of these complexes.

Complex **3**, which is based on the ligand H_2ATSM/en instead of H_2ATSM/A, showed the strongest hypoxia selectivity with an HSI value of 0.84 (at 60 min). After 1 min 15.8 ± 0.5% and 4.08 ± 0.5% had accumulated in cells under anoxic and normoxic conditions respectively, which increased to 63.6 ± 0.4% and 20.3 ± 1.9% respectively after 60 min. The increase in HSI compared to **2** results from reduced accumulation normoxic cells (anoxic uptake for both tracers was comparable). This behavior could be a result of the ethylenediamine linker group leading to a more negative Cu(I/II) redox potential in **3** compared to **1**, **2** and **4**. Previous uptake studies on *bis*(thiosemicarbazonato)Cu(II) complexes in EMT6 cells by Dearling et al. have shown a correlation between hypoxia selectivity, the Cu(I/II) redox potential and the reversibility of this reduction process, with more negative redox potentials showing the best hypoxia selectivity [30,42,48]. Close inspection of the reported data reveals that this trend is also due to the complexes with more negative redox potentials generally showing lower accumulation in normoxic cells (as opposed to greater accumulation in hypoxic cells).

As complex **3** demonstrated the most promising initial results, its cellular uptake was tested at various oxygen concentrations (Table 3). At oxygen concentrations less than 0.5% no statistically significant variation in uptake (15 min incubation) between the three concentrations measured was observed (67.2 ± 1.0%, 66.1 ± 0.9%, 64.3 ± 1.5% uptake at 0%, 0.1% and 0.5% O_2 respectively). However, at an oxygen concentration of 5%, uptake was dramatically lower (43.3 ± 1.1%). In this experiment, under normoxic conditions (20% O_2) cellular uptake of **3** was decreased further (24.1 ± 2.1%).^{64}Cu-ATSM showed higher uptake than **3** under anoxic and hypoxic conditions (92.5 ± 0.2% and 36.0 ± 0.8% respectively at 0% and 20% O_2 respectively) but displayed a lower percentage uptake than compound **3** at 5% O_2 (39.5 ± 0.9%). The results for ^{64}Cu-ATSM correspond to those obtained previously, as did the results for ^{64}Cu(acetate)$_2$ which showed minimal uptake, irrespective of oxygen concentration, and was not selective for hypoxic cells [33].

For comparison, uptake profiles of **3** and ^{64}Cu-ATSM were plotted using the ratio between the uptake of the compound at each respective oxygen concentration and the uptake of the compound under normoxic conditions against $\log_{10}$ of the oxygen concentration (Fig. 2). This analysis is preferable to using percentage uptake or HSI values since image contrast in PET ultimately depends upon the ratio of uptake between cells with a particular condition (in this case hypoxia) and those without (in this case normoxia). The plot clearly demonstrates that the ratio of normoxic to hypoxic uptake was higher for **3** than for ^{64}Cu-ATSM at all oxygen concentrations (excluding normoxia). Moreover, the uptake ratio for **3** did not change significantly from 0% to 0.5% O_2, whereas the ratio for ^{64}Cu-ATSM decreased considerably. From 0.5% to 5% O_2 the uptake ratios of both tracers decrease at a similar rate, however the high selectivity of **3** at 5% O_2 is particularly interesting. A major limitation of ^{64}Cu-ATSM is its poor delineation of mild hypoxia [46], and this is illustrated by these results which show only a 10% increase in uptake at 5% O_2 in comparison to normoxia. In contrast **3**, shows an 80% increase in uptake between the same two oxygen concentrations. These preliminary results suggest that **3** could have potential for imaging hypoxia in diseases such as cardiac ischemia which are generally associated with less severe hypoxia than the radiobiologic effect relevant to tumors [21,46].

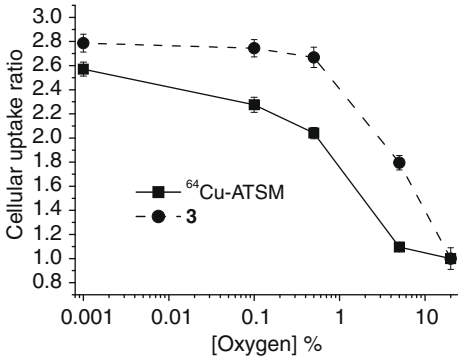

Fig. 2. Graph showing ratio of hypoxic cellular uptake to normoxic cellular uptake for compound **3** and ^{64}Cu-ATSM in EMT6 cells at varying oxygen concentrations. Errors (one stan. dev.), if not indicated, are within symbols.

3.6. Ex vivo biodistribution

Biodistribution studies were performed in BALB/c mice bearing EMT6 tumors using tracers **2** and **3** and the data obtained are shown in Table 4 (%injected dose/organ data is also provided in the supporting information). This *in vivo* model was chosen to allow qualitative comparison with the results of previous studies on ^{64}Cu-ATSM, its analogue ^{64}Cu-ATSE, the *bis*(selenosemicarbazonato)^{64}Cu complex ^{64}Cu-ASSM, and ^{64}Cu-ATSM/A imine conjugates (these studies vary only in the site and age of the implanted

Table 3
Percentage cellular uptake in EMT6 cells for **3** and ^{64}Cu-ATSM at various oxygen concentrations.

[O_2] ppm	%Cellular uptake	
	^{64}Cu-ATSM	**3**
10	92.6 ± 0.2	67.2 ± 1.0
1000	81.9 ± 1.3	66.1 ± 0.9
5000	73.5 ± 0.4	64.3 ± 1.5
50000	39.5 ± 0.9	43.3 ± 1.1
200000	36.0 ± 0.8	24.1 ± 2.1

Table 4
Biodistribution (%ID/g ± SD, $n = 4$) at 5, 20 and 60 min of **2** (top) and **3** (bottom) in BALB/c Mice Bearing the EMT6 Mammary Tumor.

Tissue	5 min	20 min	60 min
Blood	4.03 ± 0.48	3.17 ± 0.20	2.74 ± 0.17
Lung	12.6 ± 1.4	11.9 ± 1.4	11.7 ± 0.8
Liver	42.3 ± 7.2	37.9 ± 3.5	37.4 ± 5.1
Spleen	6.33 ± 1.06	5.91 ± 0.51	5.76 ± 0.88
Kidney	25.1 ± 3.9	21.1 ± 0.9	17.2 ± 1.5
Muscle	2.36 ± 0.50	1.64 ± 0.10	1.39 ± 0.20
Heart	5.55 ± 0.51	5.04 ± 0.26	4.86 ± 0.25
Brain	0.66 ± 0.09	0.71 ± 0.09	0.72 ± 0.03
Bone	1.56 ± 0.22	1.64 ± 0.18	1.94 ± 0.24
Tumor	2.17 ± 0.11	2.85 ± 0.69	2.97 ± 0.76
Intestines	8.82 ± 1.88	11.5 ± 1.1	15.3 ± 1.4
Blood	3.00 ± 0.95	2.19 ± 0.22	2.18 ± 0.68
Lung	6.10 ± 0.77	6.07 ± 0.34	6.98 ± 0.61
Liver	26.8 ± 3.7	25.9 ± 3.4	21.6 ± 0.5
Spleen	2.91 ± 0.27	2.77 ± 0.35	3.33 ± 0.33
Kidney	21.7 ± 0.4	17.0 ± 1.4	13.7 ± 0.8
Muscle	1.51 ± 0.48	1.21 ± 0.16	1.37 ± 0.26
Heart	3.03 ± 0.25	2.80 ± 0.19	3.14 ± 0.12
Brain	0.28 ± 0.06	0.26 ± 0.03	0.29 ± 0.03
Bone	1.15 ± 0.10	1.12 ± 0.18	1.37 ± 0.21
Tumor	1.68 ± 0.70	1.74 ± 0.16	2.56 ± 0.57
Intestines	18.1 ± 4.3	23.9 ± 1.6	22.7 ± 1.6

tumors) [23,33,46]. Both **2** and **3** showed rapid clearance from the blood (4.03 ± 0.48%ID/g and 3.00 ± 0.95%ID/g respectively at 5 min, decreasing to 2.74 ± 0.17%ID/g and 2.18 ± 0.68%ID/g respectively after 60 min). This is similar to all the previously reported tracers, except ^{64}Cu-ASSM which showed higher residual activity in the blood after 60 min. The general pattern of uptake in the other organs was also similar, with the liver, kidneys, intestines and lungs showing the highest levels of retention. Initial liver uptake of **2** was high (42.3 ± 7.2%ID/g at 5 min), and did not change significantly thereafter. Liver uptake of **3** was significantly lower than this (26.8 ± 3.7%ID/g at 5 min) and decreased over time (to 21.6 ± 0.5%ID/g at 60 min).

Both **2** and **3** differ from ^{64}Cu-ATSM and ^{64}Cu-ATSE, which show significantly increased accumulation in the liver over time. Hepatic clearance was observed for the ^{64}Cu-ATSM/A imine conjugates, but these appeared to give higher liver uptake than all the other tracers. The clearance of **3** from the liver is reflected in its increasing uptake in the intestines (rising from 18.1 ± 4.3%ID/g at 5 min to 22.7 ± 1.6%ID/g at 60 min). Initial intestinal uptake of **2** was considerably lower (8.82 ± 1.88%ID/g at 5 min) but also increased with time (to 15.3 ± 1.4%ID/g at 60 min). It was proposed that the high liver uptake of ^{64}Cu-ATSM/A imine conjugates could be due to their high lipophilicity and/or hydrolysis of the imine linkage. In the present study both these factors can be ruled out since hydrolysis of amides is unlikely, and **3**, which utilizes the alkylamino linker, shows lower liver uptake than **2** despite its higher log *P* value.

Accumulation of activity in the liver could occur by a number of possible mechanisms. The liver is the target organ for unchelated copper where it is trapped by metallothioneins [49]. Loss of copper from thermodynamically stable chelates via reduction and transchelation to liver enzymes has also been documented [48,50]. Parts of the liver are mildly hypoxic and high uptake has also been observed in the 2-nitroimidazole class of hypoxia markers [51,52]. The Cu(II/I) reduction process plays a direct role in the latter two mechanisms and it is therefore probable that the less negative potential and lower reversibility of this process in **2** compared to **3** results in its higher liver uptake.

The initial uptake values of **2** and **3** in the kidneys were not significantly different to each other (25.1 ± 3.9%ID/g and 21.7 ± 0.4%ID/g respectively at 5 min), but renal clearance was marginally faster for **3** (13.7 ± 0.8%ID/g at 60 min compared to 17.2 ± 1.5%ID/g for **2**). Renal clearance was also observed with ^{64}Cu-ATSM, ^{64}Cu-ATSE and ^{64}Cu-ASSM, whereas kidney uptake of the ^{64}Cu-ATSM/A imine conjugates, which at 5 min was apparently lower than all the other tracers, did not change significantly over time. The complexes also differ from each other in their lung uptake, with significantly lower%ID/g values observed for **3** in comparison to **2** (6.98 ± 0.61%ID/g and 11.7 ± 0.8%ID/g at 60 min respectively). Neither complex showed any appreciable change in lung uptake over the 60 min period. For a potential PET imaging agent it is obviously beneficial to reduce accumulation in non-target organs (i.e. the liver, intestines, kidneys and lungs), and from this point of view complex **3** is superior to complex **2**. In this case the small structural change from the H_2ATSM/A to the H_2ATSM/en backbone results in improved biodistribution characteristics. Again it is possible that the higher non-target uptake of **2** compared to **3** is due to its lesser redox stability.

In the tumor a similar level of uptake was observed for both tracers (2.97 ± 0.76%ID/g and 2.56 ± 0.57%ID/g at 60 min for **2** and **3** respectively). This appears to be lower than for ^{64}Cu-ATSM, ^{64}Cu-ATSE, and the ^{64}Cu-ATSM/A imine conjugates, and may be due to the lower lipophilicity of the nitroimidazole conjugates reducing their tissue penetration. However, it could also be a result of variations in tumor hypoxia between the different studies. In this study we were not equipped to measure the level of tumor hypoxia and therefore it is not possible to make any assessment of *in vivo* hypoxia selectivity.

4. Conclusions

Three *bis*(thiosemicarbazonato)copper(II)–nitroimidazole conjugates were successfully synthesized in their cold and ^{64}Cu radiolabelled forms. These potential combination agents for hypoxia detection showed improved hypoxia selectivity in EMT6 cellular uptake experiments when compared to a model propyl conjugate. In particular the observed difference in anoxic uptake between the 4- and 2-nitroimidazole isomers, **1** and **2**, indicates that the nitroimidazole group actively contributes to hypoxia trapping. The detailed oxygen dependent cellular uptake study carried out on **3** demonstrates that this complex is more sensitive to mild hypoxia than Cu-ATSM.

In vivo the 2-nitroimidazole conjugates **2** and **3** showed significantly different biodistributions in comparison to each other and in comparison to previously studied Cu-ATSM derivatives. Moreover uptake of the Cu-ATSM/en conjugate **3** in non-target organs was considerably lower than for the derivatives based on Cu-ATSM/A.

This study provides further evidence that a degree of control over the hypoxia selectivity and biodistribution characteristics of *bis*(thiosemicarbazonato)copper(II) complexes can be achieved by functionalisation at the exocyclic nitrogen and that the nature of both the linker and the conjugate group used have a significant impact on these properties. Future work will focus in detail on the *in vivo* hypoxia selectivity of **3** and investigate new bioconjugates based on Cu-ATSM/en.

5. Abbreviations

Boc	*tert*-butoxycarbonyl
Cu-ATSE	diacetyl-*bis*(N^4-ethylthiosemicarbazonato)copper(II)
DCC	*N*,*N*′-dicyclohexylcarbodiimide
DMF	dimethylformamide
EDC	*N*-(3-dimethylaminopropyl)-*N*′-ethylcarbodiimide
PBS	phosphate buffered saline
SCE	saturated calomel electrode
SPECT	single photon emission computed tomography
TBA	tetrabutylammonium
TFA	trifluoroacetic acid
THF	tetrahydrofuran

Acknowledgements

The authors wish to thank Nicole Fettig, Margaret Morris, Ann Stroncek, Lori Strong, and Amanda Roth for animal handling and small animal imaging support, as well as Susan Adams for cell preparation and Maria Marshall for HPLC support. Thanks also to the cyclotron facility staff and Thomas F. Voller for radionuclide production. This work was partially supported by the National Cancer Institute (R24 CA86307). We also wish to thank the British Council, CSFP, Siemens Molecular Imaging, Technology Strategy Board and Magdalen College, Oxford, for funding.

Appendix A. Supplementary material

Supplementary data associated with this article can be found, in the online version, at doi:10.1016/j.jinorgbio.2009.10.009.

References

[1] M. Hockel, P. Vaupel, J. Natl. Cancer Inst. 93 (2001) 266–276.
[2] P. Vaupel, F. Kallinowski, P. Okunieff, Cancer Res. 49 (1989) 6449–6465.
[3] C.N. Coleman, J. Natl. Cancer Inst. 80 (1988) 310–317.
[4] A.Y. Isa, T.H. Ward, C.M.L. West, N.J. Slevin, J.J. Homer, Br. J. Radiol. 79 (2006) 791–798.

[5] B.D. Clarkson, Cold Spring Harbor Conf. Cell Proliferat. 1 (1974) 945–972.
[6] M. Erlanson, E. Daniel-Szolgay, J. Carlsson, Cancer Chemother. Pharmacol. 29 (1992) 343–353.
[7] M. Wartenberg, C. Frey, H. Diedershagen, J. Ritgen, J. Hescheler, H. Sauer, Int. J. Cancer 75 (1998) 855–863.
[8] R.S. Bush, R.D.T. Jenkin, W.E.C. Allt, F.A. Beale, H. Bean, A.J. Dembo, J.F. Pringle, Br. J. Cancer 37 (1978) 302–306.
[9] R.A.K. Gatenby, H.B. Kesslerm, J.S. Rosenblum, L.R. Coia, P.J. Moldofsky, W.H. Hartz, Int. J. Radiat. Oncol. Biol. Phys. 14 (1988) 831–838.
[10] W.A. Denny, Aust. J. Chem. 57 (2004) 821–828.
[11] D.J. Honess, S.A. Hill, D.R. Collingridge, B. Edwards, G. Brauers, N.A. Powell, D.J. Chaplin, Int. J. Radiat. Oncol. Biol. Phys. 42 (1998) 731–735.
[12] W.J. Koh, K.S. Bergman, J.S. Rasey, L.M. Peterson, M.L. Evans, M.M. Graham, J.R. Grierson, K.L. Lindsley, T.K. Lewellen, K.A. Krohn, Int. J. Radiat. Oncol. Biol. Phys. 33 (1995) 391–398.
[13] R.H. Mannan, V.V. Somayaji, J. Lee, J.R. Mercer, J.D. Chapman, L.I. Wiebe, J. Nucl. Med. 32 (1991) 1764–1770.
[14] D. Sorger, M. Patt, P. Kumar, L.I. Wiebe, H. Barthel, A. Seese, C. Dannenberg, A. Tannapfel, R. Kluge, O. Sabri, Nucl. Med. Biol. 30 (2003) 317–326.
[15] D.J. Yang, S. Wallace, A. Cherif, C. Li, M.B. Gretzer, E.E. Kim, D.A. Podoloff, Radiology 194 (1995) 795–800.
[16] L.S. Ziemer, S.M. Evans, A.V. Kachur, A.L. Shuman, C.A. Cardi, W.T. Jenkins, J.S. Karp, A. Alavi, W.R. Dolbier, C.J. Koch, Eur. J. Nucl. Med. Mol. Imag. 30 (2003) 259–266.
[17] A. Brecia, B. Cavalleri, G.E. Adams (Eds.), Nitroimidazoles, Chemistry, Pharmacology and Clinical Application, Plenum, New York, 1982.
[18] G.V. Martin, J.H. Caldwell, M.M. Graham, J.R. Grierson, K. Kroll, M.J. Cowan, T.K. Lewellen, J.S. Rasey, J.J. Casciari, K.A. Krohn, J. Nucl. Med. 33 (1992) 2202–2208.
[19] A. Nunn, K. Linder, H.W. Strauss, Eur. J. Nucl. Med. 22 (1995) 265–280.
[20] S.J. Read, T. Hirano, D.F. Abbott, J.I. Sachinidis, H.J. Tochon-Danguy, J.G. Chan, G.F. Egan, A.M. Scott, C.F. Bladin, W.J. McKay, G.A. Donnan, Neurology 51 (1998) 1617–1621.
[21] E.L. Engelhardt, R.F. Schneider, S.H. Seeholzer, C.C. Stobbe, J.D. Chapman, J. Nucl. Med. 43 (2002) 837–850.
[22] Y. Fujibayashi, H. Taniuchi, Y. Yonekura, H. Ohtani, J. Konishi, A. Yokoyama, J. Nucl. Med. 38 (1997) 1155–1160.
[23] J.S. Lewis, D.W. McCarthy, T.J. McCarthy, Y. Fujibayashi, M.J. Welch, J. Nucl. Med. 40 (1999) 177–183.
[24] A.L. Vavere, J.S. Lewis, Dalton Trans. (2007) 4893–4902.
[25] F. Dehdashti, M.A. Mintun, J.S. Lewis, J. Bradley, R. Govindan, R. Laforest, M.J. Welch, B.A. Siegel, Eur. J. Nucl. Med. Mol. Imag. 30 (2003) 844–850.
[26] F. Dehdashti, P.W. Grigsby, J.S. Lewis, R. Laforest, B.A. Siegel, M. Welch, J. Nucl. Med. 49 (2008) 201–205.
[27] D.W. Dietz, F. Dehdashti, P.W. Grigsby, R.S. Malyapa, R.J. Myerson, J. Picus, J. Ritter, J.S. Lewis, M.J. Welch, B.A. Siegel, Dis. Colon Rectum 51 (2008) 1641–1648.
[28] D.I. Edwards, J. Antimicrob. Chemother. 31 (1993) 9–20.
[29] J.L.J. Dearling, J.S. Lewis, G.E.D. Mullen, M.T. Rae, J. Zweit, P.J. Blower, Eur. J. Nucl. Med. 25 (1998) 788–792.
[30] J.L.J. Dearling, J.S. Lewis, G.E.D. Mullen, M.J. Welch, P.J. Blower, J. Biol. Inorg. Chem. 7 (2002) 249–259.
[31] R.I. Maurer, P.J. Blower, J.R. Dilworth, C.A. Reynolds, Y. Zheng, G.E.D. Mullen, J. Med. Chem. 45 (2002) 1420–1431.
[32] J.P. Holland, F.I. Aigbirhio, H.M. Betts, P.D. Bonnitcha, P. Burke, M. Christlieb, G.C. Churchill, A.R. Cowley, J.R. Dilworth, P.S. Donnelly, J.C. Green, J.M. Peach, S.R. Vasudevan, J.E. Warren, Inorg. Chem. 46 (2007) 465–485.
[33] P.D. Bonnitcha, A.L. Vavere, J.S. Lewis, J.R. Dilworth, J. Med. Chem. 51 (2008) 2985–2991.
[34] S.R. Bayly, R.C. King, D.J. Honess, P.J. Barnard, H.M. Betts, J.P. Holland, R. Hueting, P.D. Bonnitcha, J.R. Dilworth, F.I. Aigbirhio, M. Christlieb, J. Nucl. Med. 49 (2008) 1862–1868.
[35] D.W. McCarthy, R.E. Shefer, R.E. Klinkowstein, L.A. Bass, W.H. Margeneau, C.S. Cutler, C.J. Anderson, M.J. Welch, Nucl. Med. Biol. 24 (1997) 35–43.
[36] C. Dardonville, C. Fernandez-Fernandez, S.-L. Gibbons, G.J. Ryan, N. Jagerovic, A.M. Gabilondo, J.J. Meana, L.F. Callado, Bioorg. Med. Chem. 14 (2006) 6570–6580.
[37] B.A. Gingras, T. Suprunchuk, C.H. Bayley, Can. J. Chem. 40 (1962) 1053–1059.
[38] Z. Li, T. Chu, X. Liu, X. Wang, Nucl. Med. Biol. 32 (2005) 225–231.
[39] M.P. Hay, W.R. Wilson, J.W. Moselen, B.D. Palmer, W.A. Denny, J. Med. Chem. 37 (1994) 381–391.
[40] H. Hirata, K. Higuchi, K. Ishikawa, S. Nakasato, Yukagaku 35 (1986) 96–101.
[41] E.K. John, M.A. Green, J. Med. Chem. 33 (1990) 1764–1770.
[42] J.L.J. Dearling, P.J. Blower, Chem. Commun. (1998) 2531–2532.
[43] H.M. Betts, P.J. Barnard, S.R. Bayly, J.R. Dilworth, A.D. Gee, J.P. Holland, Angew. Chem. Int. Ed. 47 (2008) 8416–8419.
[44] J.A. Squella, L.J. Nunez-Vergara, A. Campero, J. Maraver, P. Jara-Ulloa, J. Carbajo, J. Electrochem. Soc. 154 (2007) F77–F81.
[45] J. Carbajo, S. Bollo, L.J. Nunez-Vergara, A. Campero, J.A. Squella, J. Electroanal. Chem. 531 (2002) 187–194.
[46] P. McQuade, K.E. Martin, T.C. Castle, M.J. Went, P.J. Blower, M.J. Welch, J.S. Lewis, Nucl. Med. Biol. 32 (2005) 147–156.
[47] J.M. Brown, Int. J. Radiat. Oncol. Biol. Phys. 16 (1989) 987–993.
[48] Z. Xiao, P.S. Donnelly, M. Zimmermann, A.G. Wedd, Inorg. Chem. 47 (2008) 4338–4347.
[49] M. Yu, H. Qing, H. Guojian, Z. Shu, W. Wenqing, H. Youfeng, J.T. Kuikka, Nucl. Med. Biol. 25 (1998) 111–116.
[50] S.V. Deshpande, S.J. DeNardo, C.F. Meares, M.J. McCall, G.P. Adams, M.K. Moi, G.L. DeNardo, J. Nucl. Med. 29 (1988) 217–225.
[51] D.J. Van Os-Corby, C.J. Koch, J.D. Chapman, Biochem. Pharmacol. 36 (1987) 3487–3494.
[52] A.P. Maxwell, M.P. MacManus, T.A. Gardiner, Gastroenterology 97 (1989) 1300–1303.